Motion Deblurring Methodologies: Going Beyond Conventional Cameras

Mahesh Mohan M. R.

Guide: Prof. A. N. Rajagopalan
Image Processing and Computer Vision Lab
Department of Electrical Engineering
Indian Institute of Technology Madras

Research Motivation

- Motion blur is a common artifact in hand-held imaging.
- Apart from derailing image aesthetics, it affects most Vision tasks.

Using Blurred

Using Deblurred

Object Detection

Inputs

Using Blurred

Using Deblurred

Semantic Segmentation

Rolling shutter blurred image

Ours deblurred

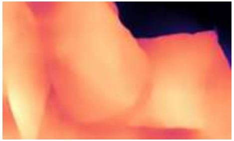

Using blurred

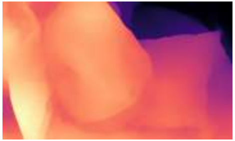

Using deblurred

Single Image Depth Estimation

Research Overview

- Present-day cameras have gone beyond Conventional Cameras.
  1. Rolling Shutter Cameras (Su et al., CVPR-15)
  2. Light Field Cameras (Srinivasan et al., CVPR-18)
  3. Unconstrained Dual-lens Cameras (*No* work exists)

- Traditional motion deblurring methods are *not* applicable for these cameras.

"Developing Suitable Motion Blur Models and Deblurring Methods."

1. Rolling Shutter Cameras
   - RS Motion Blur Model
   - Ill-posedness: RS prior
   - Unconstrained RS-BMD

2. Light Field Cameras
   - LF Motion Blur Model
   - Full-resolution LFs
   - GPU-free LF-BMD

3. Unconstrained Dual-lens
   - UDL Motion Blur Model
   - Ill-posedness: DL prior
   - Practical UDL-BMD

4. Deep Learning for UDL
   - Dynamic Scene Blur
   - View inconsistency
   - Incoherent depth

Rolling Shutter Cameras

Going Unconstrained with Rolling Shutter Deblurring; Mohan M R, A N Rajagopalan, and G Seetharaman; *ICCV 2017*

Why Rolling Shutter Cameras?

Most present-day cameras employ rolling shutter (CMOS) sensor as opposed to the traditional global shutter (CCD).

1. Higher Frame Rate

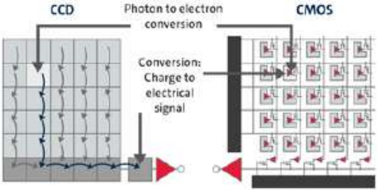

2. Longer battery life

3. Less cost

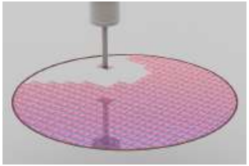

Our Objective: Rolling Shutter Deblurring

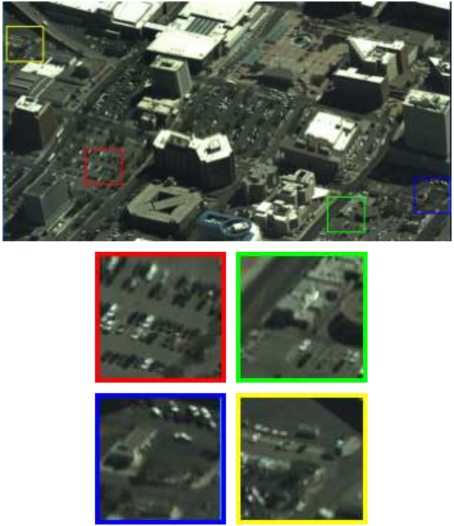

RS Blurred Image

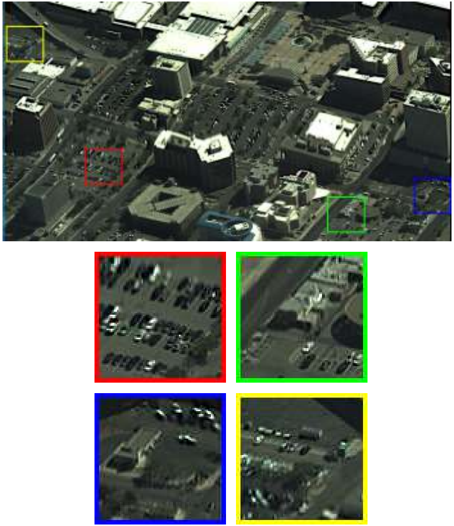

Deblurred Image

Prior Works

1. Global shutter Cameras
   - Replete with several techniques (e.g., Whyte *et al.*[1])
   - Narrow and wide FOVs via Transformation Spread Function (TSF).
   - Computationally efficient via Efficient Filter Flow (EFF).
2. Rolling Shutter Cameras (*only one* method: Su *et al.*[2])
   - Constrained to narrow FOV settings (forbids TSF).
   - Constrained to parametric camera motion.
   - Computationally expensive (forbids EFF).

[1] *Non-uniform Deblurring for Shaken Images*; Oliver Whyte, Josef Sivic, Andrew Zisserman and Jean Ponce; *IJCV 2012*
[2] *Rolling Shutter Motion Deblurring*; Shuochen Su and Wolfgang Heidrich; *CVPR 2015*

Problem Description

- In RS sensor, each row can perceive different camera motion.

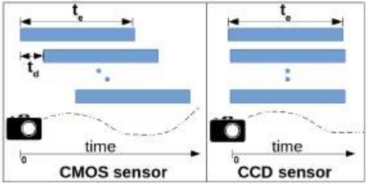

- Thus, traditional deblurring works designed for GS *fail* in RS.

Input

State-of-the-art GS deblurring

Rolling Shutter Deblurring (Su *et al.*, CVPR 2015)

Row *i*

$$= \int_{t_e^i}$$

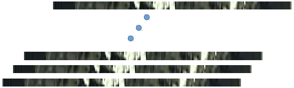

A Row of blurred image (B)

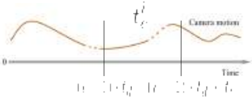

Integration of the i_{th} row of
warped versions of the clean image (L)

Rolling shutter blur model (for individual row)

$$\boxed{B^{(i)}} = \frac{1}{t_e} \int_{t=(i-1)t_d}^{(i-1)t_d+t_e} \boxed{L^{(i)}_{p(t)}} dt$$

i_{th} row of blurred Image

i_{th} row of the
clean Image warped w.r.t the ego-motion

Drawbacks of state-of-the-art RS-BMD (Su *et al.*, CVPR 2015)

Wide Field-of-View Configuration (Left - input)

Drone Imaging (Irregular camera motion)

1. Ineffective for wide-angle settings and irregular camera motion.
2. Requires precise sensor timings.
3. Computationally *very* intensive.

Central theme of Our Work (Mohan *et al.*, ICCV 2017)

GS model (*i.e.,* a single ego-motion in all image rows) includes

- both wide- and narrow-angle systems.
- both regular and irregular ego-motion.
- efficient FFT-based algorithms to relieve computational intensity.
- But not suitable for RS (since RS scanning is row-wise).

"Can we have a GS-like model suitable for RS, thereby removing constraints of the state-of-the-art."

A GS-like Model Suitable for RS

Observation: RS images can be segregated into blocks, each having a dominant ego-motion (i.e., a block-wise GS model).

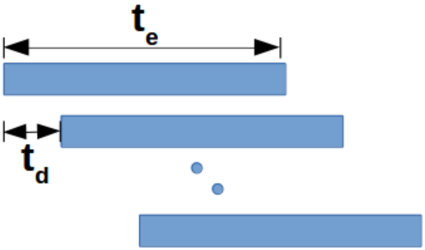

Fig: CMOS sensor timings.

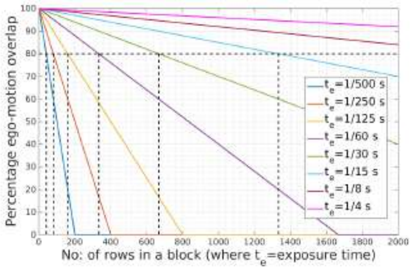

Percentage overlap with 80% overlap

The percentage camera-pose overlap in r contiguous rows is:

$$\Gamma(r) = \max\left(\frac{t_e - (r-1)\cdot t_d}{t_e}, 0\right)\cdot 100. \tag{1}$$

A GS-like Model Suitable for RS: An Example

Observation: RS images can be segregated into blocks, each having a dominant ego-motion (i.e., a block-wise GS model).

A Segregation Example: A 2240 X 1680 image with an exposure time of 1/60 s and inter-row delay of 1/100 ms.

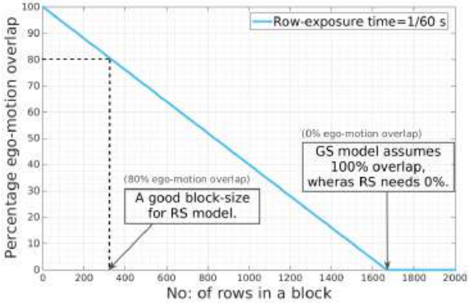

Motion blur model for RS Cameras

Thus our forward RS motion blur model is given by

$$\mathbf{B}^{l} = \sum_{p \in \mathbb{P}} w^{l}(p) \cdot \mathbf{L}_{p}^{l} \qquad : l \in \text{Individual blocks.} \tag{2}$$

How it differs from the existing RS model?

$$B^{(i)} = \frac{1}{t_e} \int_{t=(i-1)t_d}^{(i-1)t_d+t_e} L_{p(t)}^{(i)} \qquad : i \in \text{Individual rows} \tag{3}$$

1. Based on TSF.
2. Does not require a parametric camera motion.
3. Allows for computationally efficient EFF.

Challenges in RS deblurring: Spatial Aliasing

Input

Block-wise GS deblurring

Challenges in RS deblurring: Reason

Claim 1: There exist multiple solutions for the latent image-MDF pair in each individual image-block, which satisfy the forward blur model.

$$\mathbf{B}^l = \sum_{p \in \mathbb{P}} w^l(p) \cdot \mathbf{L}^l_p \qquad \text{True Solution } (\{w^l(p), \mathbf{L}^l_p\}), \tag{4}$$

$$\mathbf{B}^l = \sum_{p \in \mathbb{P}} w^l(p - p_0) \cdot \mathbf{L}^l_{p+p_0} \qquad \text{Apparent Solution } (\{w^l(p - p_0), \mathbf{L}^l_{p+p_0}\}), \tag{5}$$

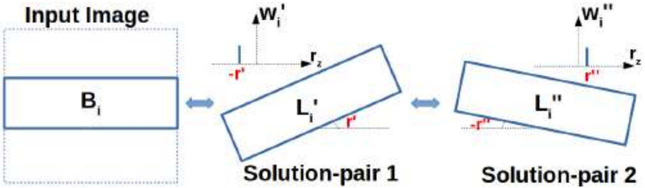

Figure: Intuition with an in-plane rotation.

Challenges in RS deblurring: Solution

Solution: A prior that nearby blocks have partially intersecting ego motion, which reduces the offset between adjacent blocks.

$$\text{prior}(\mathbf{w}) = \sum_{i=1}^{n_b} \sum_{j>i}^{n_b} \|\Gamma\left(r_b(j-i+1)\right) \cdot (\mathbf{w_i} - \mathbf{w_j})\|_2^2, \tag{6}$$

Claim 2: The prior is a convex function in **w**.

Proof Outline:

1. Eq. (10) can be represented as the l_2 norm of matrix vector multiplication, i.e., as $\|G\mathbf{w}\|_2^2$.
2. As it is a non-decreasing function (l_2) of a convex function ($G\mathbf{w}$), it must be convex.

Challenges in RS deblurring: Effect of Prior

Input

Block-wise GS deblurring

Ours (with prior)

(a) Input

(b) SotA GS-BMD

(c) SotA RS-BMD

(d) Deep Learning 1

(e) Deep Learning 2

Ours

(b- Pan et al., CVPR 2016; (c) Su et al., CVPR 2015; (d) Kupyn et al., CVPR 2018; (e) Zhang et al, CVPR 2019)

Evaluation using real camera motion (from Kohler dataset).

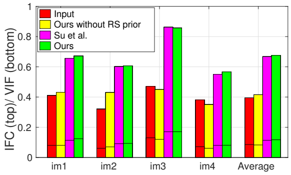

RS narrow-angle system

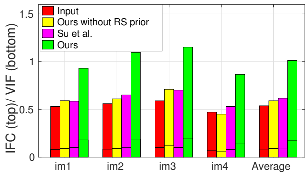

RS wide-angle system

Image dimension	Ego-motion estimation time (s)		Latent image estimation time (s)	
ht. × wd.	[24]	Ours	[24]	Ours
800×800	216.01	**29.58**	258.65	**1.44**
450×800	122.28	**22.48**	44.23	**1.30**
400×400	73.26	**10.34**	23.82	**0.62**

Computational gain over state-of-the-art (atleast 8 times speed-up)

Summary

Our work

1. Introduced a block-wise GS blur model for RS deblurring.
2. Addressed invertibility issues using a convex prior.

Our RS deblurring method

1. Allows narrow as well as wide-angle settings;
2. Accommodates irregular camera motions;
3. Eliminates the computational bottleneck of the State-of-the-art.

Light Field Cameras

Divide and Conquer for Full-Resolution Light Field Deblurring; Mohan M R and A N Rajagopalan; *CVPR 2018*

Light Field Cameras: Past to Present

From lab-based *gigantic* light field set-up [Wilburn et al., 2005]...


to consumer *hand-held* light field cameras [Ren Ng et al., 2012].

Lytro 1st generation

Lytro Illum

Raytrix

Why Light Field Cameras (over normal cameras)?

A light field image allows for *post-capture* refocusing!

Why Light Field Cameras (over normal cameras)?

A light field image allows for *post-capture* f-stopping!

Why Light Field Cameras (over normal cameras)?

3. A light field image allows for depth estimation [Tao et al. ICCV-13]

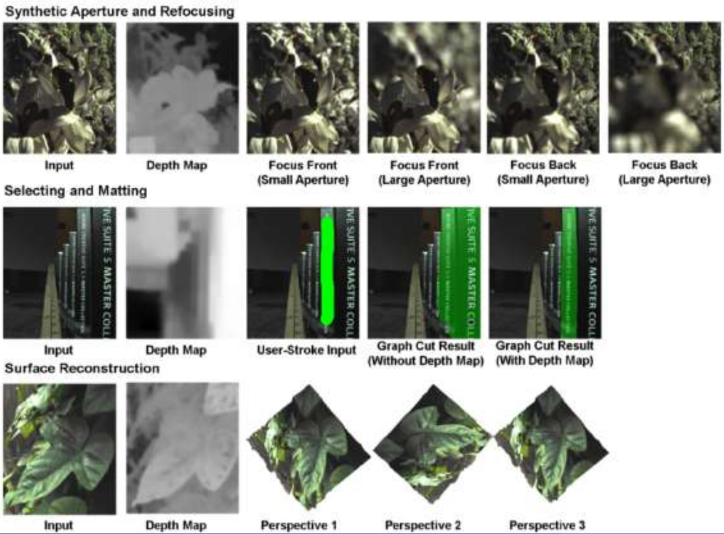

A normal image (full-aperture):

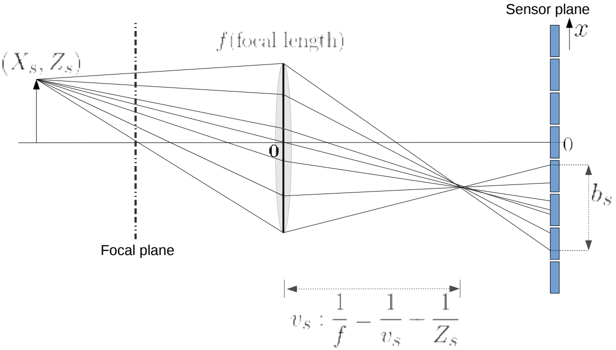

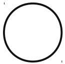

(a) Projection of a *single* scene-point

(b) Projection of an *entire* scene

Light field vs a Normal image.

A light field subaperture image (center)

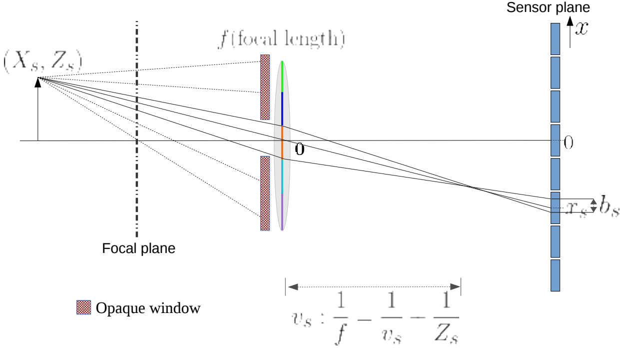

(a) Projection of a *single* scene-point for a center SA

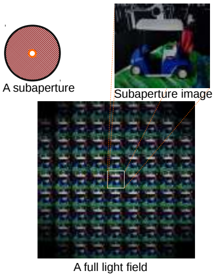

(b) Projection of an *entire* scene for a center SA

A light field subaperture image (top)

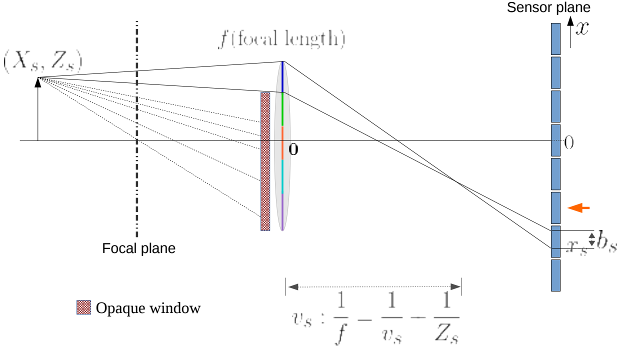

(a) Projection of a *single* scene-point for a top SA

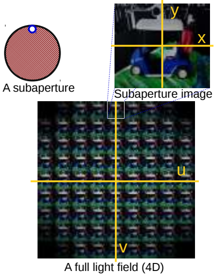

(b) Projection of an *entire* scene for a top SA

Our Objective: Light Field Deblurring

Motion blur is a common artifact in handheld photography!

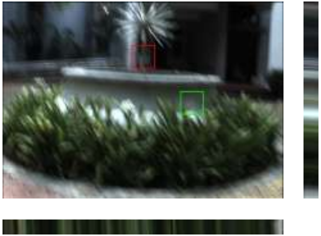

(a) Blurred light field

(b) Deblurred result

Prior Work

Prior state-of-the-art LF-BMD [Srinivasan et al., CVPR-17]

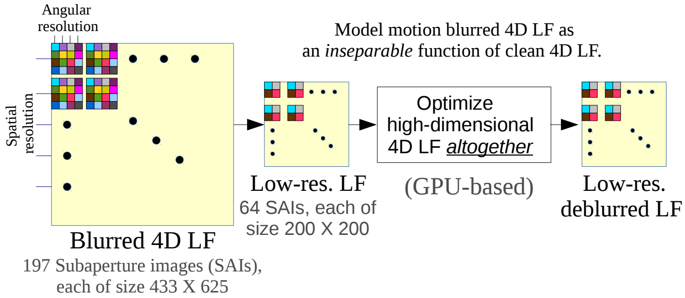

Major limitations:

- Cannot handle *full-resolution* light fields
- Necessitates *high-end GPU*.
- Cannot handle *irregular* camera motion.

Our Contributions

Prior state-of-the-art LF-BMD [Srinivasan et al., CVPR-17]

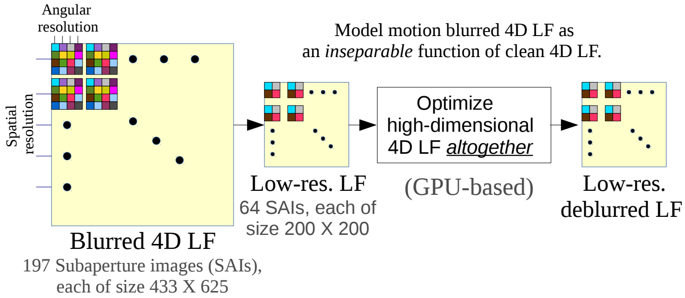

We address the limitations using a LF blur model which

- Divide Effectively
  i.e., decomposes LF-BMD into *low-dimensional* subproblems.
- CONQUER Efficiently
  i.e., enables: by solving one subproblem *reinforces* other subproblems.

Divide Effectively

A different perspective of LF blur formation:

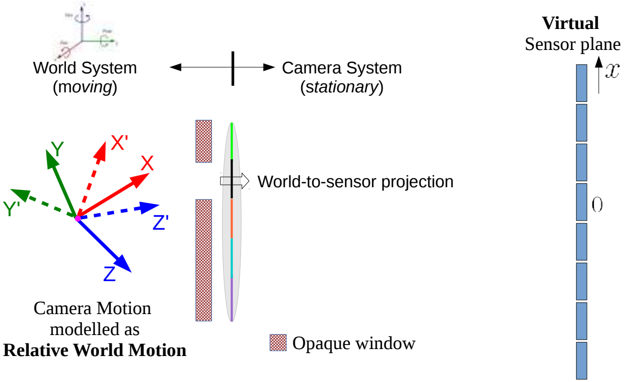

$$\underbrace{B_i}_{i\text{th blurred SAI}} = \sum_{p \in \mathbb{P}} \underbrace{\omega_p}_{TSF} \cdot \underbrace{F_i(R_p \mathbf{X})}_{\text{W-to-S of } i\text{th SAI}}, \text{ where } F_i(\mathbf{X}) \text{ is the } i\text{th clean SAI.} \quad (7)$$

Divide Effectively

World-to-sensor projection for the ith SA image (F_i):

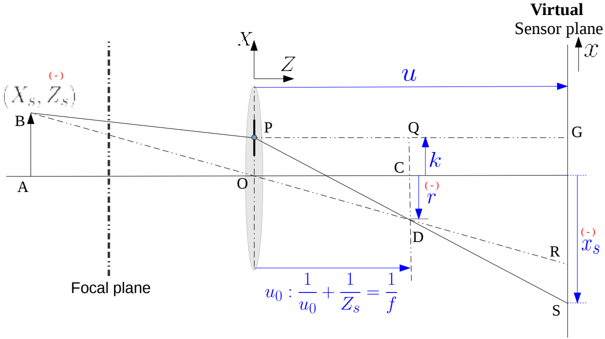

$$\begin{bmatrix} x_s \\ y_s \\ 1 \end{bmatrix} = \frac{1}{Z_s} \begin{bmatrix} u & 0 & k_x(f-u)/f \\ 0 & u & k_y(f-u)/f \\ 0 & 0 & 1 \end{bmatrix} \begin{bmatrix} X_s \\ Y_s \\ Z_s \end{bmatrix} - \frac{1}{Z_s} \begin{bmatrix} k_x u \\ k_y u \\ 0 \end{bmatrix} \tag{8}$$

Divide Effectively

Cases for scene-points *behind* the focal-plane:

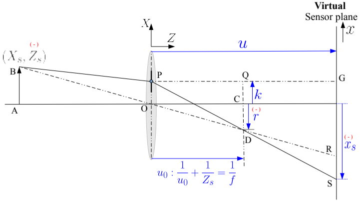

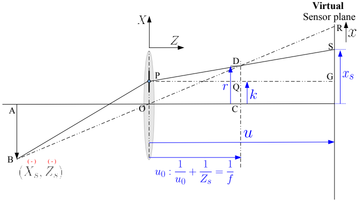

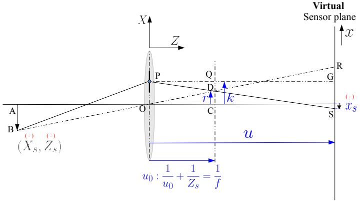

Cases for scene-points *in front* of the focal-plane:

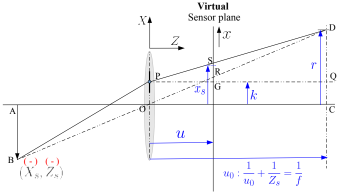

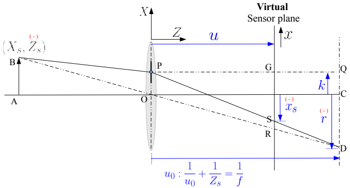

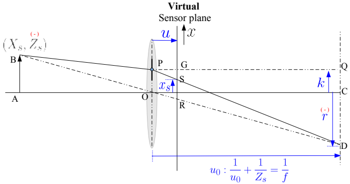

Divide Effectively

$$\boxed{\underbrace{B_i}_{i\text{th blurred SAI}} = \sum_{p\in\mathbb{P}} \underbrace{\omega_p}_{TSF} \cdot \underbrace{F_i(R_p\mathbf{X})}_{\text{W-to-S of } i\text{th SAI}}, \; 1 \leq i \leq N.} \tag{9}$$

Light field deblurring:

1st SA image $\rightarrow$ AM for (5,5) iterations to estimate $\{\underbrace{F_1(X)}_{\text{1st deblurred SAI}}, \omega_p\}$

$\vdots$

ith SA image $\rightarrow$ AM for (5,5) iterations to estimate $\{\underbrace{F_i(X)}_{i\text{th deblurred SAI}}, \omega_p\}$

$\vdots$

Nth SA image $\rightarrow$ AM for (5,5) iterations to estimate $\{\underbrace{F_N(X)}_{N\text{th deblurred SAI}}, \omega_p\}$

Lytro Illum has 197 SAIs!

Conquer Efficiently

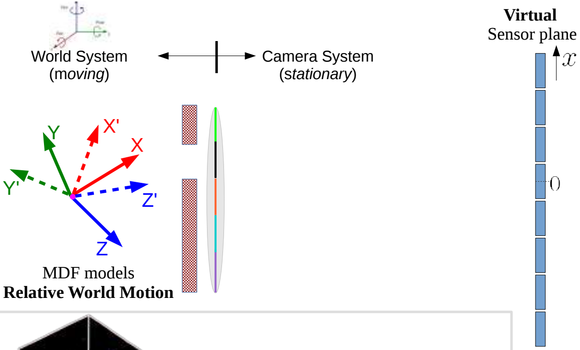

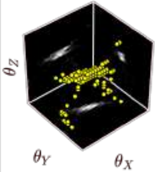

The MDF is *independent* of camera-parameters.

So, do we need to estimate it again and again? No.

Conquer Efficiently

$$\boxed{\underbrace{B_i}_{i\text{th blurred SAI}} = \sum_{p\in\mathbb{P}} \underbrace{\omega_p}_{TSF} \cdot \underbrace{F_i(R_p\mathbf{X})}_{\text{W-to-S of } i\text{th SAI}}, \; 1 \leq i \leq N.} \tag{10}$$

Light field deblurring:

1st SA image $\rightarrow$ AM for (5,5) iterations to estimate $\{\underbrace{F_1(X)}_{\text{1st deblurred SAI}}, \omega_p\}$

$\vdots$

ith SA image $\rightarrow$ *one-shot* non-blind method to obtain $\{\underbrace{F_i(X)}_{i\text{th deblurred SAI}}\}$

$\vdots$

Nth SA image $\rightarrow$ *one-shot* non-blind method to obtain $\{\underbrace{F_N(X)}_{N\text{th deblurred SAI}}\}$

(For Lytro Illum, a cost improvement of $197\times$ *for camera-motion estimation and* $5\times$ *for latent image estimation.)*

Outline of our method

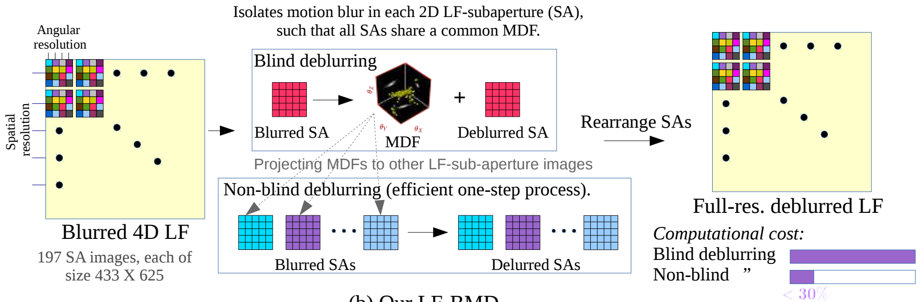

(b) Our LF-BMD

The major limitations of the state-of-the art method were:

- Cannot handle *full-resolution* light fields.
- Necessitates *high-end GPU*.
- Cannot handle *irregular* camera motion.

Results

Computational cost:

LF-resolution $\{x, y, u, v\}$	State-of-the-art **(GPU-based)**	Ours **(CPU-based)**
$\{200, 200, 8, 8\}$	2 hrs, 20 mins	8.21 mins (Gain $\mathbf{17.05}\times$)
$\{200, 289, 8, 8\}$ (Low-res. LF)	3 hrs, 17 mins	12.62 mins (Gain $\mathbf{15.61}\times$)
$\{433, 625, 15, 15\}$ **(Full-res. LF)**	Not feasible (Resource allocation error)	38 mins* **(Feasible)**

* Parallelized in 8 cores of a CPU. Using more cores or GPU further improves the speed significantly.

Results

Full-resolution Light field:

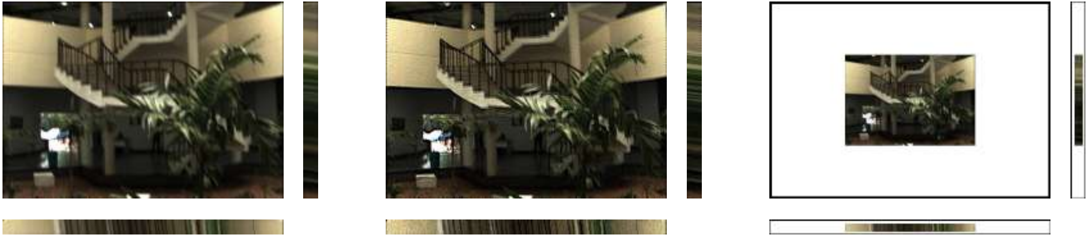

(a) Blurred light field (b) Ours (c) Srinivasan et al. CVPR-2017

Results

Irregular camera motion:

(a) Blurred light field

(b) Ours

(c) Srinivasan et al. CVPR-2017 + Bilinear interpolated

Summary

We have seen LF blur in a *different* perspective, which:

1. Initiated the first ever solution for full-resolution LF deblurring;
2. Allows computationally efficient LF deblurring (even *sans* GPU);
3. Caters to irregular ego-motion.

“As LF cameras continue to evolve with higher resolutions, we believe that the divide and conquer strategy will be invaluable for full-resolution deblurring”.

.

Unconstrained Dual-lens Cameras

Unconstrained Motion Deblurring for Dual-lens Cameras; Mohan M R, Sharath Girish, and A N Rajagopalan; *ICCV 2019*

Why Unconstrained dual-lens Cameras?

A DL camera captures *depth information* to enable many applications.

Unconstrained DL Cameras

Image

Depth

Segmentation

Portrait Photography

Binocular or 3D Vision

Scene Understanding

Unconstrained Dual-lens Cameras?

Two cameras **need not** share the **same** configuration.

Examples of unconstrained DL cameras

1. Focal lengths
   - Same: Binocular or 3D vision.
   - Different: Capture narrow, wide, or wider field-of-views.
   - Full-overlap: Super-resolution and visual odometry.
   - Differently exposed: HDR imaging, low-light photography, and stereoscopics.
2. Can have different image resolutions.

Our objective: Motion Deblurring in Unconstrained DL Cameras

Motion deblurring with *scene-consistent* disparities.

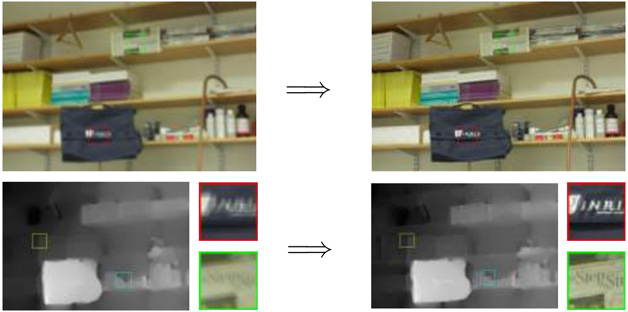

Input   Output

Prior Works

Motion deblurring is unexplored in unconstrained DL set-ups.

1. Constrained DL deblurring is *not* applicable here (Su et al., CVPR 2019[3]).

2. Challenges (w.r.t. conventional camera deblurring)

    (-) Deblurring has to ensure scene-consistent disparities.

    (-) Popular narrow-FOV: Amplifies blur and center-of-rotation effect.

    (-) Handle more than one image: Higher dimensional optimization.

[3] *Davanet: Stereo deblurring with view aggregation*; Zhou, S., J. Zhang, W. Zuo, H. Xie, J. Pan, and J. S. Ren; *CVPR 2019*

Our Contributions

*"Motion blur model for unconstrained dual-lens?
Can direct deblurring preserves scene-consistent disparities?"*

Our work

1. Introduces a generalized dual-lens blur model.
2. Reveals an ill-posedness that disrupts consistent disparities.

Our method

1. Ensures scene-consistent disparities via a DL prior;
2. Accommodates arbitrary center-of-rotation;
3. Admits a low-dimensional deblurring approach.

Generalized Dual-lens Motion Blur model

Motion blurred image is a combination of multiple warped images.

$$\mathbf{I}_B^n = \sum_{p \in \mathbb{P}^3} w^n(p) \cdot P^n\Big(R_p(\mathbf{X} - \mathbf{l_c}) + \mathbf{l_c} + \mathbf{l_b}\Big)\, dp, \tag{11}$$

$\mathbf{I}_B^n \rightarrow$ blurred image $\quad$ $\mathbf{l_c} \rightarrow$ COR $\quad$ $\mathbf{l_b} \rightarrow$ base-line $\quad$ $\mathbb{P}^3 \rightarrow$ Camera pose-space

$w^n(p) \rightarrow$ proportion of time camera stayed in pose p $\quad$ $P^n(\cdot) \rightarrow$ World-to-sensor projection

Projection P^n is derived as

$$\mathbf{x}' = \lambda\Big(\mathbf{K}^n\mathbf{R}(\mathbf{K}^n)^{-1}\mathbf{x} + \underbrace{\frac{1}{Z}\mathbf{K}^n(\mathbf{I} - \mathbf{R})\mathbf{l_c}}_{\text{center-of-rotation}} + \underbrace{\frac{1}{Z}\mathbf{K}^n(\mathbf{I} - \mathbf{R})\mathbf{l_b}}_{\text{baseline}}\Big). \tag{12}$$

"Motion blur in a DL set-up is depth-variant due to the baseline and COR."

Challenges in Unconstrained DL-deblurring

Claim 1: There exist *multiple valid* solutions of deblurred image-pairs, but that produce scene-inconsistent disparities.

$$\begin{aligned}\mathbf{I}_B^n &= \sum_p w^n(p)P^n\Big(R_p(\underbrace{\mathbf{X}}_{true}-\mathbf{I_c})+\mathbf{I_c}+\mathbf{I_b}\Big),\\ &= \sum_p w^n(p)P^n\Big(R_pR_n^{-1}\big(\underbrace{R_n(\mathbf{X}-\mathbf{I_c})+\mathbf{I_c}}_{apparent}-\mathbf{I_c}\big)+\mathbf{I_c}+\mathbf{I_b}\Big), \quad \forall R_n.\end{aligned} \tag{13}$$

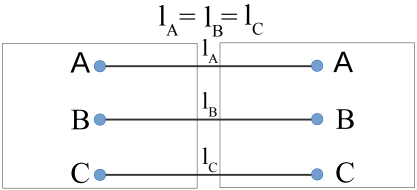

(a) True solution

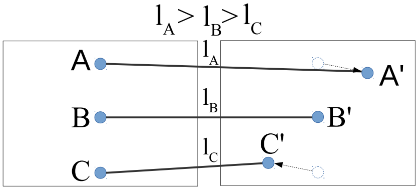

(b) An apparent solution (inplane rotation)

A new prior for Unconstrained DL Motion Deblurring

Ill-posedness is due to *relative* shifts among individual MDFs.

$$\text{DL Cost} = \underbrace{\text{Image-pair cost}}_{\text{Convex}} + \underbrace{\text{MDF-pair cost}}_{\text{Convex, \underline{Not} interdependent}} + \underbrace{\|\mathbf{w}^n - \mathbf{w}^w\|_2}_{\text{DL Prior}}. \tag{14}$$

The prior *curbs* the relative shifts among individual MDFs.

Claim 2: The DL prior is convex, and when added to the deblurring cost retains the biconvexity property. Also, the prior allows for efficient LASSO optimization (i.e., $\arg\min_{\mathbf{w}} \|\mathbf{K}\mathbf{w} - \mathbf{b}\|_2^2 : \|\mathbf{w}\|_1 \leq \lambda$)

Implication of the Ill-posedness and Prior

The prior curbs the relative shifts among individual MDFs.

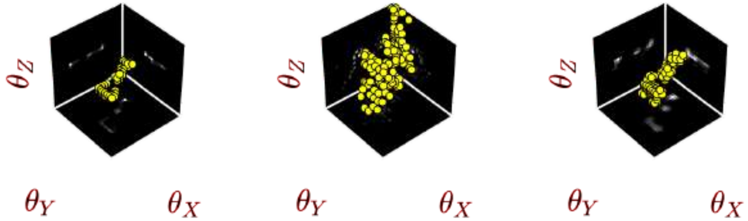

(a) True MDF (b) *Without* prior (c) With DL prior

(1) True patches (2) *Without* DL prior (3) With DL prior

A practical algorithm for Unconstrained DL Deblurring

We show that a multi-lens deblurring problem can be:

1. divided into *subproblems*;
2. instilled with the proposed *prior* and biconvexity property;
3. solved using *AM* for COR, depth, MDFs, and images.

Results

PSNR (dB)	Blur	W/o Prior W/o COR	W/o Prior W/ COR	W/ Prior W/o COR	W/ prior W/ COR
Image	22.39	25.69	26.59	27.28	28.88
Depth	28.33	23.35	**23.59**	29.12	**30.52**

The DL prior reduces the ill-posedness by a good margin (i.e., by 7 dB, as indicated in bold).

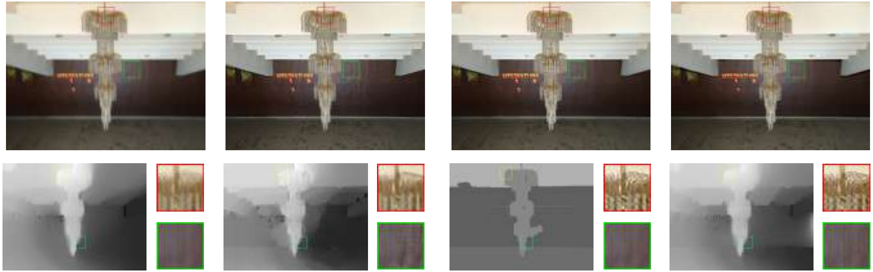

Real inputs SL Deep (ICCV-17) SL Depth (CVPR-14) Our result

Summary

As a first, we address the motion blur problem in Unconstrained DL cameras:

1. Introduced a generalized motion blur model;
2. Revelaled and addressed an inherent ill-posedness that distorts depth cues;
3. A practical algorithm for presentday Unconstrained DL cameras.

Unconstrained Dual-lens Cameras (Dynamic Scene Blur)

Unconstrained Motion Deblurring for Dual-lens Cameras; Mohan M R, Sharath Girish, and A N Rajagopalan; *ICCV 2019*

Dynamic Scene Deblurring for Unconstrained DL Cameras

Apart from camera motion, motion blur occurs due to dynamic objects as well.

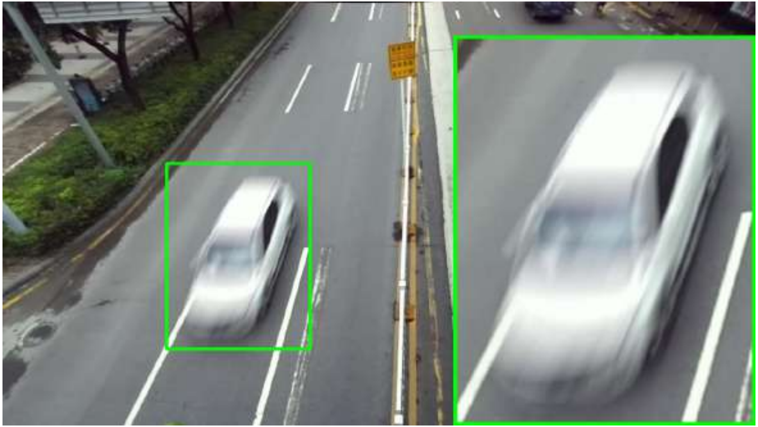

(Note that dynamic scene blur is highly space-variant).

Prior Works

Dynamic Scene Motion deblurring is unexplored in unconstrained DL set-ups.

1. Constrained DL deblurring is *not* applicable here (Xu et al., ICCP 2014).
2. The DL prior in [Mohan et al., ICCV 2019] does not work for dynamic case.
3. DL deep learning work (Su et al., CVPR 2019) admits several challenges
    - (-) Disrupt view-consistency in DL images.
    - (-) Does not enforce scene-consistent disparities.
    - (-) Deblurring is not space-variant and image-dependent.

Stereoscopics require left-right views to be coherent.

Input (patches of left-right views inset)

Existing method (Davanet, CVPR 2019)

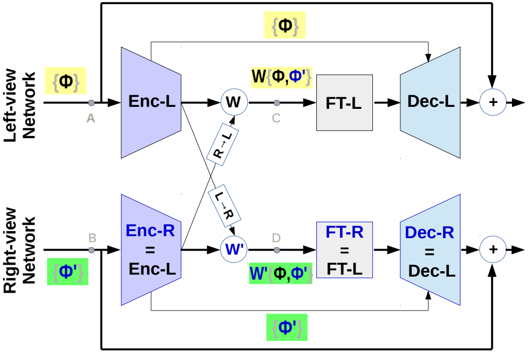

View-inconsistency Solution: Coherent Fusion Module

Equalizes signal flow in left-right node-pairs.

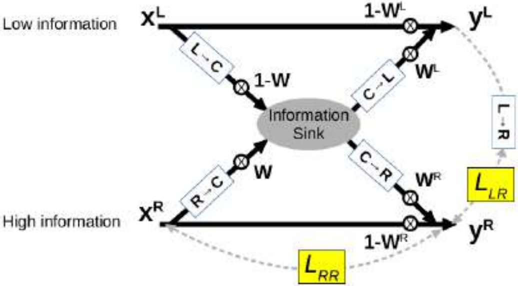

Left-view (more degradation)

Right-view)

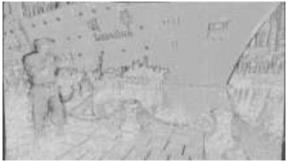

Mask of right-view

Problem of Scene-inconsistent Depth

In a stereo set-up, one view sees a different time instant as that of the other view.

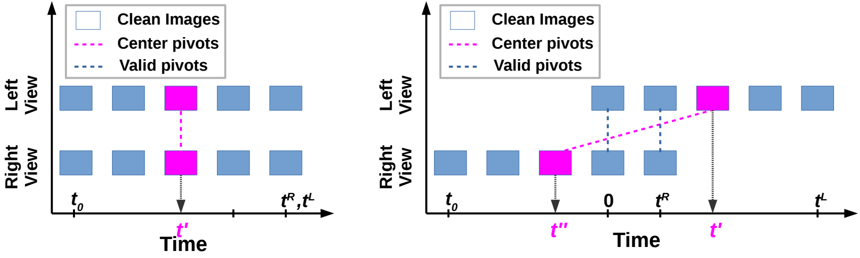

(a) Constrained case (b) Unconstrained case

Blur becomes lesser at lower scales, and so is the depth inconsistency.

Adaptive Scale-space for Scene-inconsistent Depth

Depth of scale-space network has to adapt with depth inconsistencies.

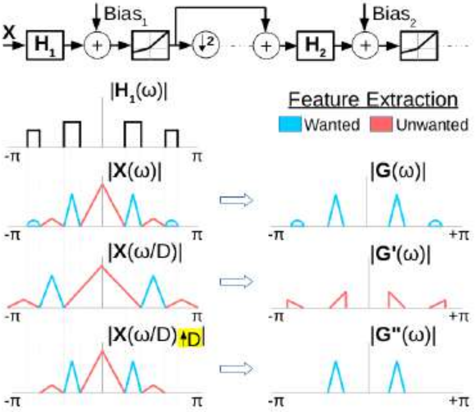

(a) Transforming fine to coarse network

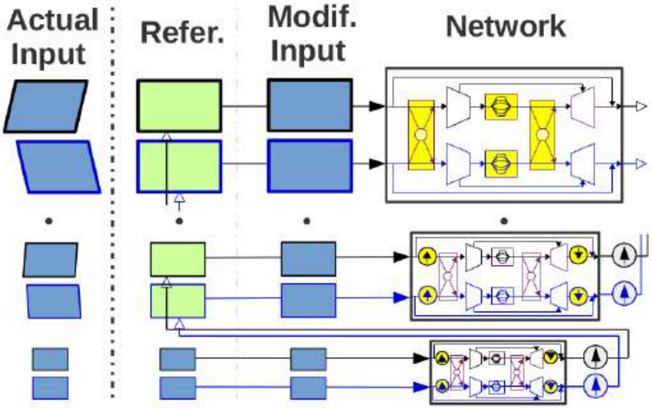

(b) Adaptive scale-space network

Filter realizations adapt to spatial coordinates.

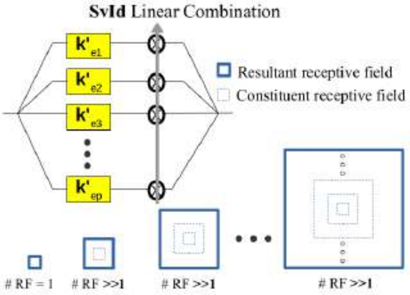

SvId Module

1(a) Blurred I/p | 1(b) RF 3×3 ($r = 1$) | 1(c) RF 5×5 ($r = 2$) | 1(d) RF 7×7 ($r = 3$) | 1(e) RF 9×9 ($r = 4$)

Quantitative Results

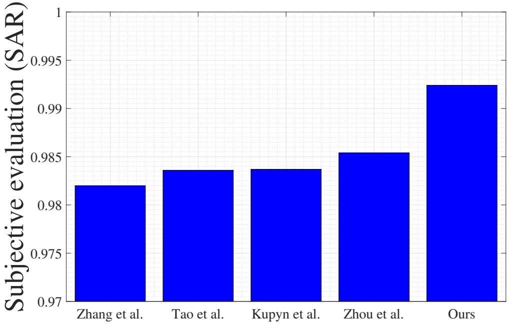

(a) SAR metric (for view-consistency)[4]

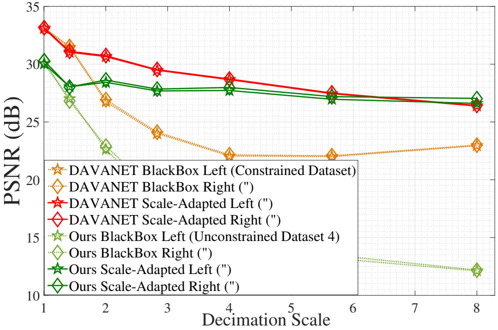

(b) Adaptive scale-space results

[4] *Full-reference quality assessment of stereopairs accounting for rivalry*. A C Bovik et al., 2011, Signal processing: Image Communication

Qualitative Results

Input

Unconstrained DL (ICCV-2019)

DAVANET (CVPR-2019)

Ours

Summary

Effective modules for Deep Learning for unconstrained DL based on Signal Processing:

1. Coherent Fusion Module to address View-inconsistency;
2. Adaptive Scale-space approach to address Depth-inconsistency;
3. SvId module for Space-variant Image-dependent deblurring.

"Our coherent fusion module can be potentially applied for diverse deep learning applications with unconstrained DL. Adaptive scale-space approach enables extending diverse deep networks for lower image-scales.".

.

Conclusions

We addressed motion deblurring for cameras that span beyond Conventional Cameras

1. Deblurring model, Prior, and Method for Rolling Shutter Cameras;
2. Divide and Conquer strategy for Light Field cameras;
3. Introduced Motion Deblurring approach for Unconstrained DL Cameras.
4. Learning based Dynamic Scene Deblurring for Unconstrained DL Cameras

Publications based on the Thesis

1. Going Unconstrained with Rolling Shutter Deblurring.
   Mahesh Mohan M. R., Rajagopalan A. N., and Gunasekaran Seetharaman.
   In Proceedings of the *International Conference on Computer Vision*
   (**ICCV 2017**), IEEE Publications, Pages 4010–4018.
2. Divide and Conquer for Full-Resolution Light Field Deblurring.
   Mahesh Mohan M. R. and Rajagopalan A. N.
   In Proceedings of the *Conference on Computer Vision and Pattern Recognition*
   (**CVPR 2018**), IEEE Publications, Pages 6421–6429.
3. Unconstrained Motion Deblurring for Dual-lens Cameras.
   Mahesh Mohan M. R., Sharath Girsih, and Rajagopalan A. N.
   In Proceedings of the *International Conference on Computer Vision*
   (**ICCV 2019**), IEEE Publications, Pages 7870–7879.

Under Review

- Scale-adaptive Coherent-fusion for DL Dynamic Scene Deblurring.
  Mahesh Mohan M. R., Nithin G. K., and Rajagopalan A. N.
  IEEE Transactions in Image Processing.